



HAL
open science

Quantifying hydro-sedimentary transfers in a lowland tile-drained agricultural catchment

Thomas Grangeon, Valeria Ceriani, Olivier Evrard, Aurélie Grison, Rosalie Vandromme, Arthur Gaillot, Olivier Cerdan, Sébastien Salvador-Blanes

► To cite this version:

Thomas Grangeon, Valeria Ceriani, Olivier Evrard, Aurélie Grison, Rosalie Vandromme, et al.. Quantifying hydro-sedimentary transfers in a lowland tile-drained agricultural catchment. *CATENA*, 2021, 198, pp.105033. 10.1016/j.catena.2020.105033 . cea-03011226

HAL Id: cea-03011226

<https://cea.hal.science/cea-03011226v1>

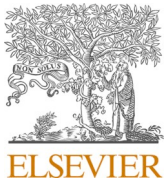
Submitted on 18 Nov 2020

HAL is a multi-disciplinary open access archive for the deposit and dissemination of scientific research documents, whether they are published or not. The documents may come from teaching and research institutions in France or abroad, or from public or private research centers.

L'archive ouverte pluridisciplinaire **HAL**, est destinée au dépôt et à la diffusion de documents scientifiques de niveau recherche, publiés ou non, émanant des établissements d'enseignement et de recherche français ou étrangers, des laboratoires publics ou privés.

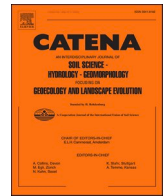


Distributed under a Creative Commons Attribution 4.0 International License



Contents lists available at ScienceDirect

Catena

journal homepage: www.elsevier.com/locate/catena

Quantifying hydro-sedimentary transfers in a lowland tile-drained agricultural catchment

Thomas Grangeon^{a,*}, Valeria Ceriani^b, Olivier Evrard^b, Aurélie Grison^c, Rosalie Vandromme^a, Arthur Gaillot^{a,d}, Olivier Cerdan^a, Sébastien Salvador-Blanes^d

^a Bureau de Recherches Géologiques et Minières, Département Risques et Prévention, 3 Avenue Claude Guillemin, Orléans, France

^b Laboratoire des Sciences du Climat et de l'Environnement (LSC-IPSL), UMR 8212 (CEA/CNRS/UVSQ), Université Paris-Saclay, Gif-sur-Yvette, France

^c Syndicat Mixte du Bassin versant de la Bonnée, 8 Place du Martroi, Saint-Benoit-sur-Loire, France

^d EA 6293 GéHCO - Université de Tours, Faculté des Sciences et Techniques, Tours, France

ARTICLE INFO

Keywords:

Soil erosion
Suspended sediment transfers
Tile drainage

ABSTRACT

Soil erosion, runoff and sediment connectivity are strongly impacted by anthropogenic features in lowland agricultural catchments. Among these landscape features, the role played by tile drainage on water and sediment transfers and hillslope-to-river connectivity in drained catchments remains poorly understood. This study quantified water and sediment transfers in a tile drained catchment of central France by combining high frequency rainfall, discharge and sediment concentration measurements at the outlet of a set of 10 tile drained plots (34 ha) and at the medium-sized (120 km²) catchment scale. Over the monitoring period, including a dry and a wet year compared to average conditions (one year with 112% of the mean annual rainfall and one year with 64% of the mean annual rainfall), 36 rainfall-flood events were recorded and analyzed. The high frequency analysis of water and sediment transfers in tile-drained plots showed a high seasonal variability and the occurrence of two transfer pathways in the soil column including the slow drainage of saturated soils and the occurrence of preferential flow pathways through the soil column. Indeed, 13 of the 36 recorded flood events showed hydrographs with two components, reflecting these two pathways: slow transfers in the soil columns and fast transfers through soil macropores and/or cracks. Indeed, at the beginning of the flood event, a high-magnitude peak overlaid on the hydrograph. On average, this fast peak contributed 15% of the water and sediment fluxes. The sediment dynamics in tile drains was suggested to depend on sediment storage and exhaustion processes occurring in the tile drain network.

1. Introduction

In Europe, agricultural landscapes were strongly modified following WWII to increase agricultural productivity through the removal of hedges, land consolidation and stream redesigning programs (Souchère et al., 2003; Evrard et al., 2010). The agricultural areas were also extended in lowland areas with the installation of tile drainage systems to convert wetlands into arable land. A review conducted by Montagne et al. (2009) demonstrated that these changes may act as geomorphic agents, which outlines the need to consider their role in catchment sediment dynamics. Installing tile drainage systems may have extensive environmental implications (Blann et al., 2009) because they may increase transfers of sediments from plots to rivers, which may have deleterious impacts on downstream environments (Owens et al., 2005;

Kemp et al., 2011). Indeed, tile drainage creates new pathways for water, sediment and associated pollutants resulting in the loss of on-site nutrients such as phosphorous (Ulén and Persson, 1999; Macrae et al., 2007; Ulén et al., 2012). Furthermore, tile drains may also lead to off-site impacts including the enhanced export of pesticides (Kladivko et al., 2001). A specific problem occurring in these drained systems is associated with the fact that fluxes occurring in tile drains may bypass soil conservation measures (e.g. grass buffer strips) designed to prevent runoff and sediment transfers from cultivated land to the river channel (Le Bissonnais et al., 2004). These fluxes are therefore directly delivered to the river systems, resulting in an increased connectivity between plots and river systems, which may directly affect the water quality (Roze-meijer et al., 2010). Moreover, it was demonstrated that a direct connection between the soil surface and tile drainage systems may occur

* Corresponding author.

E-mail address: t.grangeon@brgm.fr (T. Grangeon).

<https://doi.org/10.1016/j.catena.2020.105033>

Received 27 March 2020; Received in revised form 24 October 2020; Accepted 2 November 2020

0341-8162/© 2020 The Authors. Published by Elsevier B.V. This is an open access article under the CC BY license (<http://creativecommons.org/licenses/by/4.0/>).

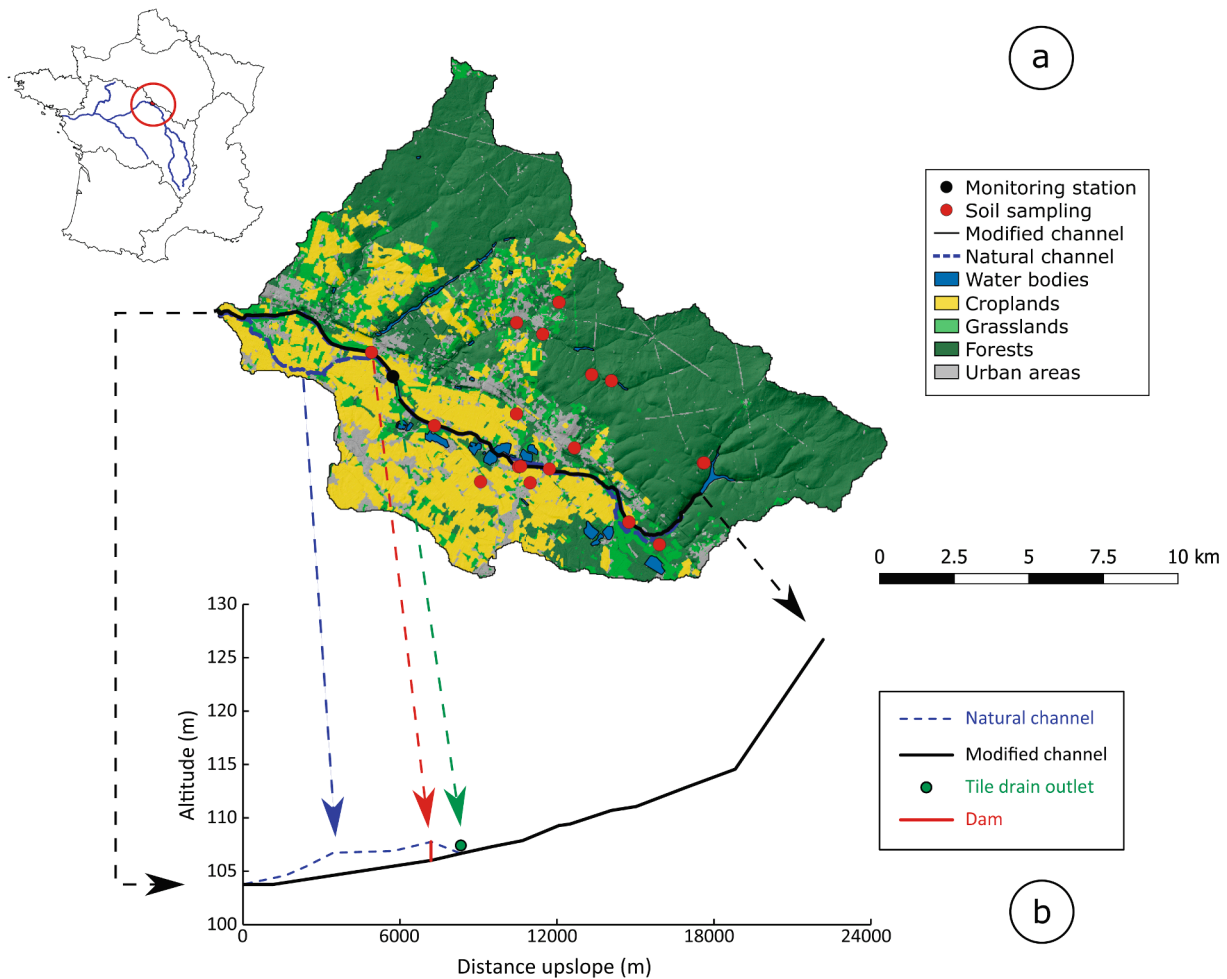


Fig. 1. a) Location of the Bonnée River catchment with its confluence with the Loire River. The situation of hydrological monitoring stations and soil sampling locations is indicated with the black and red dots, respectively. Land use data were extracted from Corine Land Cover (2018). b) Longitudinal view of the main river bed. Both the original and modified river channels are indicated. (For interpretation of the references to color in this figure legend, the reader is referred to the web version of this article.)

(Akay and Fox, 2007; Frey et al., 2016), resulting in the limited retention and degradation of contaminants within the soil column (Stone and Wilson, 2006).

So far, most studies dealing with water and sediment transfers from tile drainage have been conducted at the plot scale (e.g. Turunen et al., 2013; Muma et al., 2016). They demonstrated that suspended sediment concentrations in subsurface drain flows could exhibit large variations and represent a large proportion of sediment fluxes (Deasy et al., 2009). Experimental studies were designed to investigate this issue both in the field and in the laboratory (e.g. Turtola et al., 2007; Van Den Bogaert et al., 2013). For instance, Uusitalo et al. (2001) measured concentrations ranging from 540 to 1240 mg.l⁻¹. Chapman et al. (2005) measured concentrations up to 2600 mg.l⁻¹. Based on this extensive research, very detailed numerical models were developed to simulate water and sediment transfers in drained plots (Warsta et al., 2013; Turunen et al., 2017). However, the role of preferential flows in the transfers of water, associated fertilizers and pesticides in drained systems remains unclear (Nagy et al., 2020a, 2020b). Moreover, the upscaling of these results from the plot to the catchment scales remains unresolved to date (De Vente and Poesen, 2005; Evrard et al., 2008; Delmas et al., 2012; Fiener et al., 2019). There is a lack of quantitative assessments of the impacts of tile drainage on water and sediment fluxes at the catchment scale, despite the fact that previous studies outlined the need to monitor drained catchments in order to improve our understanding of these preferential transfer pathways (Li et al., 2010; Hansen et al., 2013; King

et al., 2014).

Previous studies investigating sediment transfers in tile drained catchments mainly relied on sediment fingerprinting approaches (Russell et al., 2001; Walling et al., 2002; Walling and Collins, 2008; Foucher et al., 2015; Le Gall et al., 2017). This technique consists in the measurement of conservative properties in potential sources and in sediment collected in the main river to quantify the respective contributions of these potential sources to the material transiting the river (Haddachi et al., 2013; Collins et al., 2017). They demonstrated that contributions from tile drains may be very variable, even at the flood event scale. However, these studies often combined tile drains with other sediment sources (e.g. channel banks in Cooper et al., 2015 or surface cropland in Foucher et al., 2015), underlining the complexity and the variety of processes involved in sediment transfers from tile drains.

In contrast, very few studies quantified water and sediment transfers from tile drains at the catchment scale based on high resolution (<15-minutes time step) drain and river monitoring, although the importance of quantifying these fluxes at very detailed temporal resolutions was demonstrated in contrasted environmental contexts (Meybeck et al., 2003; Navratil et al., 2011; De Girolamo et al., 2015). Although King et al. (2014) quantified water transfers from multiple tile drains with a high temporal resolution and evaluated their contribution to the entire catchment water budget, they did not measure suspended sediment fluxes. Cooper et al. (2015) combined high temporal resolution rainfall and water monitoring with sediment fingerprinting to construct time

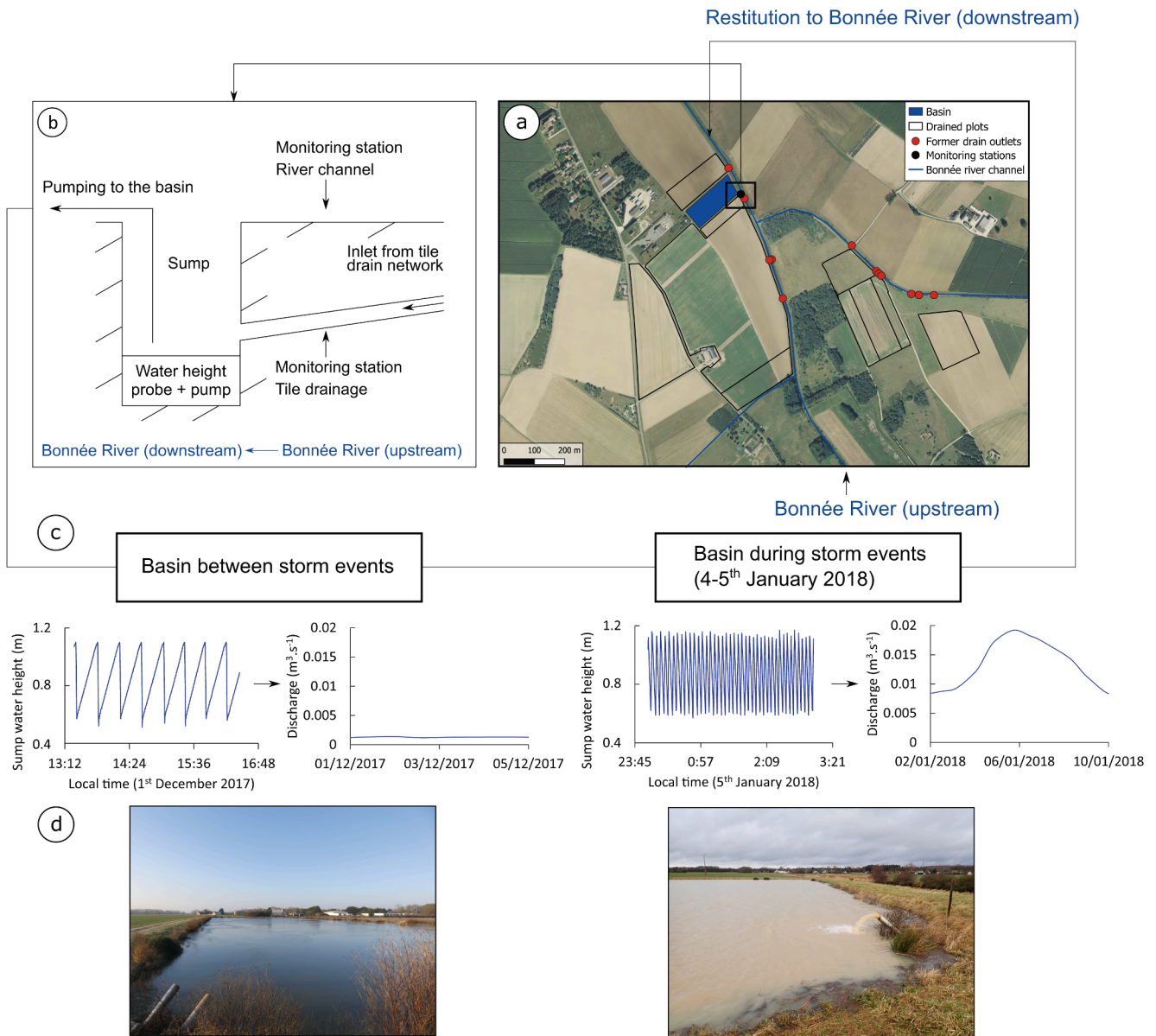


Fig. 2. a) Zoom on the localization of the monitoring stations. Note that the pipes originating from the eastern plots cross the Bonnée river. b) Fluxes from the tile drain network are collected in a sump, which is monitored with a water height probe. They are then pumped into a basin (lower panel) and then delivered to the main Bonnée river network. c) The water height in the sump was used to calculate discharge from the tile drain network. d) Pictures of the pumping outlet and basin. They were taken during high and low flows and illustrate the observed variations in turbidity from the tile drain network.

series of tile drain contributions. They however restricted their analysis to eight rainfall events only and did not quantify sediment fluxes with a high frequency. Grangeon et al. (2017) quantified water and sediment dynamics with a high temporal resolution at both the drained plot and the catchment scales, in an area where 41% of the surface is drained. They measured concentrations ranging from a few to $1600 \text{ mg}\cdot\text{l}^{-1}$, and estimated fluxes from tile drains to represent 0–63% of the catchment fluxes, with a mean of 13%. They also hypothesized that sediment fluxes mainly consisted of the flush of material stored in channels, but did not analyze the potential sediment storage in tile drains. However, their analysis was restricted to data from a single tile drain, which may lead to representativity issues and prevent the extrapolation of their results to larger and/or contrasted catchments. The objective of the current study was therefore to analyze the tile drain functioning, based on a set of drained plots to increase the analysis representativity. In particular, the processes leading to the seasonal and flood event scale variations in water and suspended sediment dynamics will be analyzed. To this end,

water and suspended sediment dynamics at the outlet of multiple tile drains were monitored with a high temporal resolution (10 minute time step) over two contrasted hydrological years.

2. Materials and methods

2.1. The Bonnée River catchment

The Bonnée catchment is a medium-sized (120 km^2 at the monitoring station) headwater catchment tributary of the Loire River (France), mainly covered with cropland and forest.

Forest dominates in catchment upper parts while lower parts are mainly covered with cropland (Fig. 1a). Wheat, maize, sugar beet, rapeseed and sunflower are the main crops cultivated in the region. The tile drained area is ranging from 30% to 50% of the utilized agricultural land in this part of France (Tourné et al., 2020; Vincent, 2020). Elevation ranges from 103 to 176 m. Catchment topography is mainly

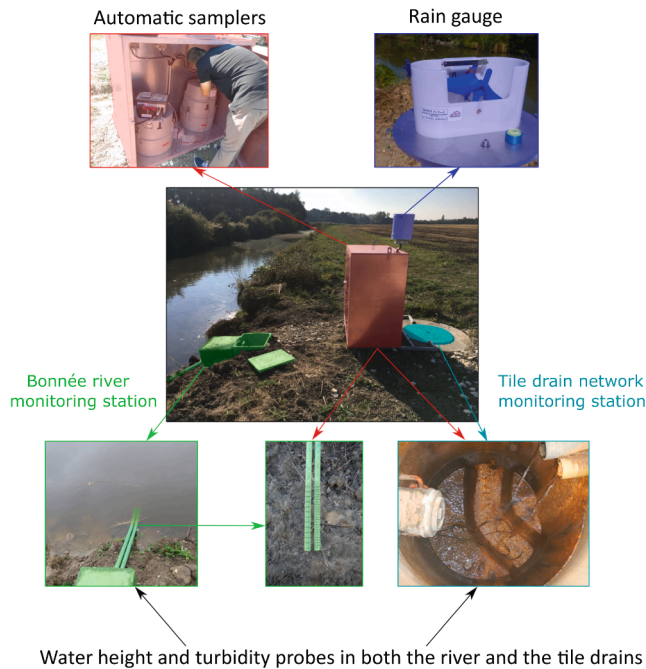


Fig. 3. Hydro-sedimentary monitoring stations in the tile drain network and the Bonnée River. The distance between the two stations is approximately 4 m.

composed of a sequence of three plateaus, separated by steeper gradient steps: slope first, fifth (median) and ninth deciles amount to 0.3%, 1.7% and 7.1%, respectively, calculated from a 5-m resolution DEM. Highest slopes are mainly found in upper parts, under forests. Soils are mainly sandy and clayey and are developed on alluvial deposits. The climate is temperate (Cfb) according to the Köppen-Geiger climate classification (Peel et al., 2007; Beck et al., 2018) with mean monthly temperatures ranging from 3 °C to 18 °C. The mean annual rainfall amounts to 637 mm at the nearby Orléans station, according to the national weather service, based on 30-year records (1981–2010). Monthly means are ranging from 45 mm to 65 mm, with higher values recorded from October to December and in May, and lower values recorded during summer.

2.2. River channel redesigning and tile drain network

The river channel was channelized between 1960 and 1970. The goal was to reduce the water transfer time to the outlet to decrease soil saturation, increase the agricultural productivity and reduce the inundation risk (Spaling and Smit, 1995). Consequently, the original (i.e. natural) river channel was disconnected (the natural water channel became higher than the redesigned one) and abandoned. To redirect the water flow into the original river channel and initiate the ecological restoration of the river to comply with the European Water Framework Directive, a small dam built between 1960 and 1970 was enhanced (up to 1.90 m) in 2013 (Fig. 1b).

It increased the water height in the upstream river section and resulted in water flowing both within the natural and the redesigned channels. However, it also increased the water height above some of the tile drains outlet, which made them inoperative. Therefore, a unique manmade, sewer-like network was installed to allow tile drain functioning, collecting water flowing from a set of 10 fields equipped with tile drains, covering a surface area of 34 ha (Fig. 2a). At the outlet of this network, water and sediment were collected in a sump (Fig. 2b). They were then pumped up into a wetland in order to trap sediment and contaminants before supplying ‘clean’ water to the river network. This sewer network therefore completely isolated tile drain fluxes from the river flow, providing a unique opportunity to monitor water and

sediment fluxes from a set of tile drained cultivated fields during both baseflow and flood events.

Tile drain characteristics were variable across the set of fields monitored in the current research. They were all made of perforated PVC pipes. The pipe diameters ranged from 45 to 700 mm, and they were buried between 30 cm and 1.8 m below the soil surface.

2.3. Hydrological monitoring station

Two monitoring stations were installed to measure the water and sediment fluxes in both the Bonnée River and in the tile drain network. The river station was installed next to the tile drain network (Fig. 3) and was located 1 km upstream of the dam.

Each station was equipped with a water height (Nivelco Nivopress NKK) and a turbidity probe (Neotek Ponsel, 0–4000 NTU). An automatic sampler (Teledyne ISCO 3700) was used to collect river water and suspended sediment samples, mainly during flood events. An automatic pluviometer (Précis Mécanique 3029) was installed to monitor rainfall. Water height, turbidity and rainfall were monitored with a 10-minute resolution from September 2017 to July 2019. Because of several technical problems (e.g. probe failures), only the period from December 2017 to July 2019 was investigated in the current research.

2.3.1. Water discharge measurements in the main river

In the river, 11 streamflow measurements were performed during low and high flow periods in order to derive relationships to convert water height into discharge. However, a simple least square regression between water height and discharge did not allow fitting the relationship. High flows were underestimated, which was problematic because they transport most of the sediment fluxes (Navratil et al., 2011). A non-linear fitting procedure taking into account streamflow measurement uncertainties was therefore developed and resulted in a rating curve able to capture the highest discharges. The detailed procedure and the corresponding rating curve are provided as [supplementary material](#).

When the highest storm event occurred (mid-February 2017 and during a large event in July 2018), the dam was opened by the local authorities to prevent flooding. In both cases, the water height time series was linearly interpolated when the dam was opened. The water height time series was not considered for analysis in February 2017. In July 2018, as the dam opening was performed during the falling limb of the hydrograph, the event was considered for analysis.

2.3.2. Water discharge measurements at the tile drain network outlet

Because of a low water height in the tile drain network and limited probe resolution (respectively in the order of 1–10 cm with 1 cm resolution), water height was measured in the sump, collecting fluxes from the entire tile drainage network. Due to fast water height variations, especially during flood events, it was monitored with a 15-second time step. The water volume time series in the sump, resulting from both tile drain network discharge and the sump pumping, was estimated from water height time series using the well-defined geometry of the sump (Fig. 2c). The volume calculated during the rising limb provided water input from the tile drain network, while the falling limb (resulting from pumping) were removed. Consequently, the discharge time series was calculated for rising limb periods and interpolated across pumping periods (Fig. 2). The resulting discharge time series was then interpolated at a 10-minute time step to match the recording time step of the other measurements.

2.4. Soil and sediment sampling and analysis

2.4.1. Suspended sediment sampling and analysis

Suspended sediment was sampled using the ISCO 3700 device based on water level thresholds and time intervals during flood events, both in the tile drain network and in the Bonnée river. This procedure was adapted based on the monitored water level before a forecasted flood

event. In general, it consisted of one sampling per hour when the water level increased by more than 5 cm. The sampled water volume was fixed at 500 ml, although small (± 10 ml) variations were measured. Therefore, the volume was systematically measured in the laboratory. River water was filtered with 0.45 μm -mesh filters and oven-dried at 105 °C for 24 h to obtain suspended sediment concentrations. These measurements were used to establish a suspended sediment concentration-turbidity rating curve. It was used to convert turbidity into suspended sediment concentration time series. The turbidity-concentration relationship was good for the Bonnée river and the tile drain network ($R^2 = 0.93$, $n = 93$ and $R^2 = 0.88$, $n = 44$, respectively). The sample concentrations were comprised between 8 and 3100 $\text{mg}\cdot\text{l}^{-1}$ for the Bonnée river. Due to technical issues (flood event flashiness and noise on the raw measured turbidity), sample concentrations for the tile drain network varied between 3 and 210 $\text{mg}\cdot\text{l}^{-1}$. Consequently, the concentration was extrapolated for less than 6% of the monitoring period.

2.4.2. Soil surface observations

Finally, during the two-year monitoring period, a monthly visual inspection of the soil surface was performed on the drained plots to document the density of the soil cover by vegetation, crusting stage, surface roughness and the occurrence of soil cracks, as all these characteristics were shown to control the runoff and erosion behavior of cultivated plots (Cerdan et al., 2002).

2.5. Flood event separation

Flood events were defined according to the methodology presented in Grangeon et al. (2017). Flood events were identified based on the ratio between quick flow and base flow (calculation based on the methodology proposed by Chapman, 1991). The correspondence of flood events occurring both in the tile drain network and in the main river was verified. Then, single storm events were defined as events cumulating more than 1 mm precipitation. Flood events were then associated with rainfall events, and when multiple storm events were recorded during a single flood event, they were grouped into a single event. This procedure resulted in a dataset of 36 coupled storm-flood events occurring in both the river and the tile drain network between December 2017 and June 2019. The following analysis is based on these 36 flood events, although some supplementary individual events were recorded only in the Bonnée River or in the tile drain network.

2.6. Data analysis

For these 36 individual flood events, several characteristics were calculated including rainfall depth (mm), duration (h), mean and maximal intensity ($\text{mm}\cdot\text{h}^{-1}$), flood event volume (m^3), total, rising and falling limb durations (h), mean and maximal discharge ($\text{m}^3\cdot\text{s}^{-1}$), runoff coefficient (%), antecedent rainfall (rainfall depth cumulated over the previous 48 h, mm), mean and maximal concentration ($\text{mg}\cdot\text{l}^{-1}$), sediment load (kg). Specific peak discharge was calculated by dividing the peak discharge by the catchment or tile drain network area. Sediment loads were obtained through the integration of the product of the water discharge and the sediment concentration time series.

Results were considered separately for winter (December to February), spring (March to May), summer (June to August) and autumn (September to November). A correlation matrix using Pearson correlation coefficients was used to analyze the statistical relationships between these variables.

The statistical analysis will be used to investigate (i) the tile drainage network dynamics and (ii) the global catchment dynamics.

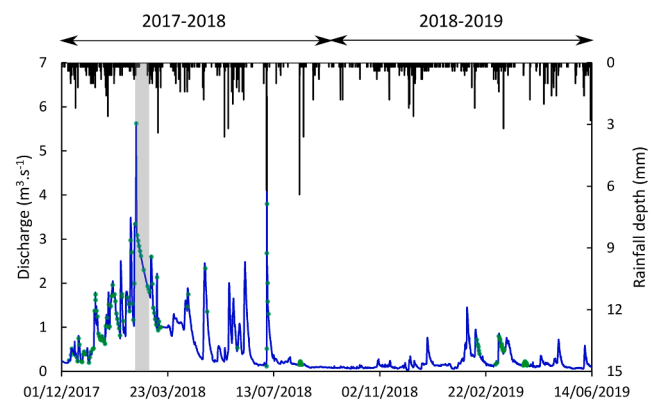


Fig. 4. Rainfall (black line) and water discharge (blue line) recorded at the Bonnée River monitoring station between 2017 and 2019. The green dots correspond to the suspended sediment samples collected using the ISCO sampler. The gray area corresponds to a period of dam opening; data for this period were not considered. Hydrological years are indicated with arrows in the upper part of the figure. (For interpretation of the references to color in this figure legend, the reader is referred to the web version of this article.)

3. Results and discussion

3.1. Rainfall and river catchment dynamics

During the monitoring period, two contrasted hydrological years (defined as years starting on September 1st) were recorded (Fig. 4).

The 2017–2018 hydrological year concentrated most of the rainfall and flood events. Moreover, during the monitoring period, most of the storm events occurred in winter and in spring (Table 1). From 1st January to 31st March the total rainfall amounted 254 mm, corresponding to 162% of the long-term average over the same period (157 mm).

These floods contributed 60% and 83% of the annual water fluxes in the river and the tile drain network, and 62% and 92% of the sediment fluxes. The flashiness of the water and sediment fluxes was previously demonstrated for headwater catchments (e.g. Navratil et al., 2011) and for tile drained areas (King et al., 2014; Grangeon et al., 2017), underlining the importance of conducting a high resolution monitoring in these systems.

Of note, heavy rainfall was observed in July 2018 after a dry period: only 7 mm was recorded in the previous 3 weeks. More than 42 mm was then recorded in less than 6 h. At a 10-minute time step, the maximum rainfall intensity reached 37 $\text{mm}\cdot\text{h}^{-1}$. This event generated a significant flood event, even leading to the flooding of a nearby village (located about 10 km away from the monitoring station), and corresponding to the highest peak discharges observed throughout the entire study period. This event suggested the occurrence of infiltration-excess overland flow in this lowland medium-sized catchment.

Furthermore, the river baseflow remained at a high level during 2017–2018, especially during winter (62% of the annual total water fluxes). This high contribution from baseflow underlines the high soil moisture levels observed during this period of long-lasting and continuous rainfall, also characterized by a low evapotranspiration. Accordingly, discharge from tile drains was high during this period. Moreover, eight flood events occurred during winter following low rainfall amounts (< 10 mm), while flood events were never triggered by such a low rainfall amount during the other seasons. These observations, combined with the distribution of rainfall and the number of flood events recorded during seasons and over the monitoring period, indicated that this period was prone to saturation-excess runoff.

Although a quantitative study of the relative importance of infiltration- and saturation-excess could not be performed because of the lack of monitoring data across the entire catchment, this information,

Table 1

Main hydrological characteristics of the monitored period. The flood event percentage is relative to the entire monitoring period (2017–2019).

Hydrological year	Recorded rainfall (mm) – Percentage of the long term average (%)	Flood events recorded over the monitoring period (number-percentage)	Winter flood events during the hydrological year (number- percentage)	Spring flood events during the hydrological year (number-percentage)	Autumn and summer flood events during the hydrological year (number-percentage)
2017–2018	716 mm – 112%	23–64%	14–61%	7–30%	2–9%
2018–2019	408 mm – 64%	13–36%	6–46%	3–23%	4–31%

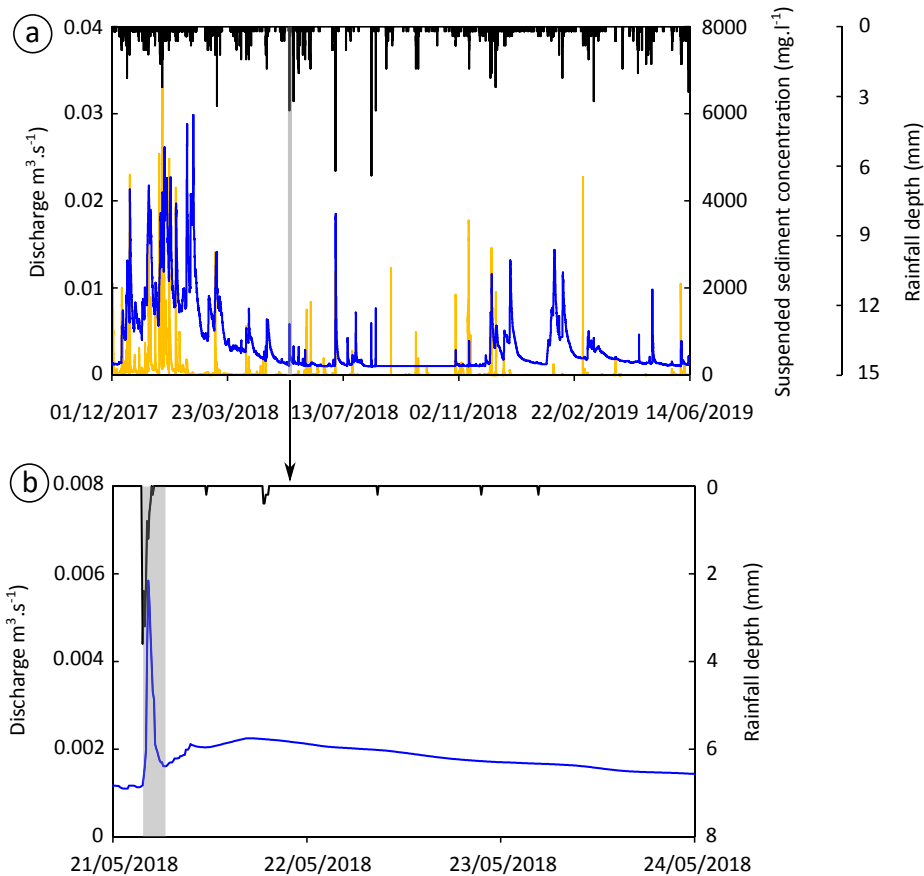


Fig. 5. a) Rainfall and discharge time series measured at the outlet of the tile drainage network. b) A zoom on the situation observed during a flood event that started on 21st May 2018 illustrates the behavior of discharge during an individual flood event with the successive occurrence of fast, as illustrated by the gray shaded area, and slow discharge stages.

combined with the calculation of the water balance (calculation provided in the [supplementary material](#)), demonstrated that both

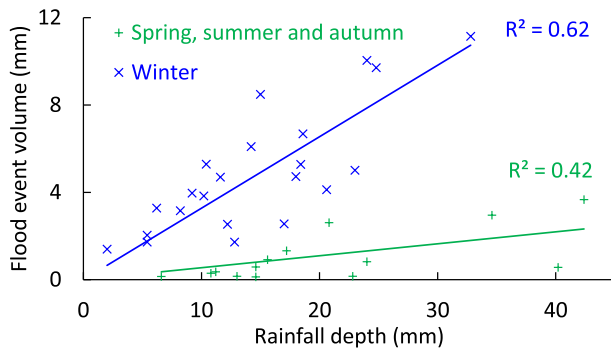


Fig. 6. Relationships between rainfall depth and the water volume during the 36 identified flood events for the tile drainage network, for winter (blue) and the other seasons (green). (For interpretation of the references to color in this figure legend, the reader is referred to the web version of this article.)

infiltration- and saturation-excess processes were involved in flood generation in the study area. This interpretation is in line with the findings of [Saffarpour et al. \(2016\)](#) and [Grangeon et al. \(2017\)](#), although the current research suggested their combined occurrence at a much larger scale. The occurrence of soil saturation in a drained catchment had important implications on the hydrological regime and on flow occurrence in the tile network. It will also affect sediment connectivity across the catchment by allowing runoff, and therefore sediment transport, to occur more regularly and to take place on parts of the hillslopes that would not be prone to infiltration-excess runoff.

3.2. Tile drainage network water dynamics

A constant low flow ($\approx 1 \times 10^{-3} \text{ m}^3 \cdot \text{s}^{-1}$) was observed and measured over the entire monitoring period in the tile drainage network ([Fig. 5a](#)).

It reflected the constant inflow of water from a local spring. As the corresponding discharge was constant and low, with the absence of suspended sediment in the flow, it was considered negligible in this study. In 2017–2018, tile drainage water discharge exhibited much higher values, the 25th decile of the discharge time series was 75%

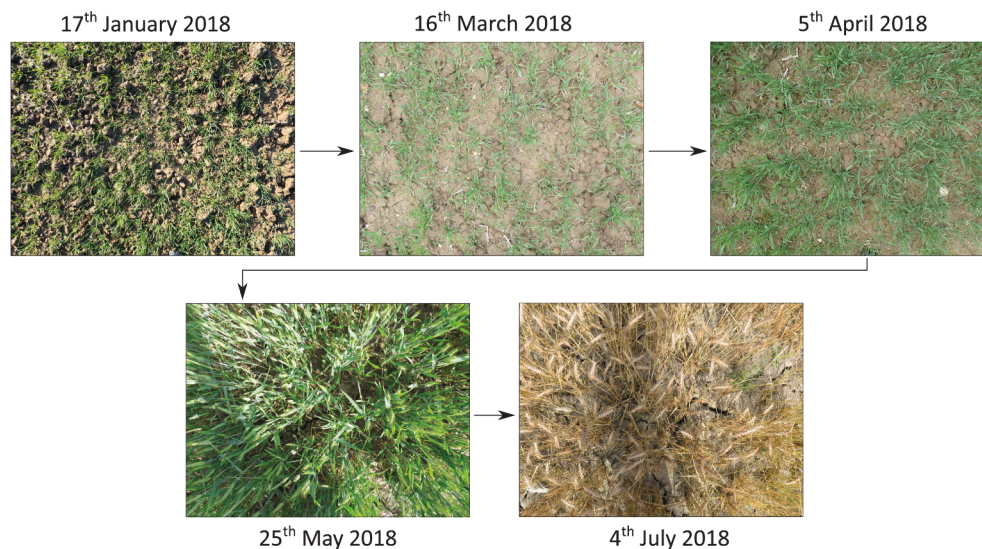


Fig. 7. Progressive development of soil cracks on one of the studied drained plots. Cracks progressively developed from the end of winter to become fully developed in summer.

higher in 2017–2018 (up to $0.03 \text{ m}^3 \cdot \text{s}^{-1}$) compared to discharges recorded in 2018–2019 (up to $0.02 \text{ m}^3 \cdot \text{s}^{-1}$). In 2017–2018 and, to a lesser extent, in 2018–2019, base flow was generated during winter and spring because of the high soil moisture content, which was progressively evacuated by tile drains, both during and between storm events. Moreover, flows from tile drains increased during rainfall events, in direct relation with rainfall depth. Consequently, most of the flood events (64%) were recorded during the 2017–2018 hydrological year. The quick response of the tile drainage flow to rainfall suggests the occurrence of a direct connection between the soil surface and the rest of the soil column, increasing water and sediment vertical connectivity across the soil profile. On the contrary, late in spring and during summer, transfers from the tile drainage system were ephemeral, with successive periods of low and high flows, corresponding to highly variable transfers and connectivity levels across the soil column.

Although a link was found between the discharged volume from tile drains and the rainfall depth (Fig. 6), two relationships had to be derived for winter, on the one hand, and the remaining seasons, on the other hand.

R^2 amounted to 0.62 and 0.42, respectively, and both regressions were significant at the 5% level. This result reflects the seasonal behavior of tile drain systems in the study area, despite the relatively high connectivity maintained throughout the entire year between soils and the drain network. This seasonal behavior reflects variations in the soil surface properties (e.g. soil crusting may prevent water infiltration into the soil, although in this study, infiltration capacity could not be measured), the sparse soil cover by vegetation as observed through qualitative soil surface observations (Fig. 7) and the low temperatures. Indeed, all of these factors directly influence the soil moisture content.

During rainfall events, a quick response of discharge was observed in the tile drainage network throughout the monitoring period (Fig. 5b, the quick flow is highlighted by the gray shaded area). A peak in the discharge time series was regularly measured, and overlaid on the rising limb of floods occurring during the soil saturation period. When focusing on the 36 identified flood events, 13 of them were characterized by the occurrence of two clearly different peaks, as illustrated in Fig. 5b, in both time and magnitude: a rapid and high-magnitude peak occurring at the beginning of the event overlaying on the global, longer and lower flood signal. Overall, 46% of the flood events displaying this double peak occurred during spring and 38% occurred in summer. As they were mainly recorded during spring and summer, this quick flow component is assumed to be controlled by flow occurring in soil macropores and

shrink-swell cracks, which is in line with the results of previous studies (Kladivko et al., 1991; Øygarden and Jenssen, 1997). This hypothesis was also confirmed by field observations made during the current research (Fig. 7).

It is also possible that these peaks did occur in winter, although they were diluted by the higher magnitude of the winter flood events. Quantifying precisely the contribution of these two peaks over multiple hydrological conditions would provide an interesting perspective for future research.

In addition to these coupled river-tile drain flood events, 12 other events displaying this quick discharge component were measured in the tile drains only. All these events were observed during spring and summer. Our results demonstrated that, in addition to transfers triggered by soil saturation, preferential flow occurring through soils cracks and macropores may occur in the soil column. Various flow conditions and connectivity levels in the tile drains were therefore observed throughout the year. This result may have an important impact on the transfer time of water, sediment and the associated contaminants. Stone and Wilson (2006) previously measured this type of behavior in the US (Indiana) at the outlet of a single tile drain from a unique field, during two flood events. They demonstrated the important implications of these preferential flows, accounting for 11% to 51% of the total flood flow, on glyphosate transfers. Our study demonstrates, using high frequency and long time series that these preferential flows occur frequently. Moreover, their occurrence was confirmed at larger scales (multiple drained fields and flood events) and in another environmental context, suggesting that it may be a generalized behavior of tile drainage. On average, at the flood event scale, preferential flow (occurring through macropores and cracks), calculated as the volume measured during the fast peak relative to the total flood volume, supplied 10–15% of the water fluxes to the total tile drainage network. It was estimated by isolating this peak on the hydrograph and calculating the relative water volume, compared to the total flood event volume. Therefore, the substances applied to the fields may be transferred with these preferential flows to the river channel with limited effects of soil retention and degradation.

3.3. Tile drainage suspended sediment dynamics and transfers to the river

The dynamics of suspended sediment concentrations from tile drains were very episodic and they displayed a contrasted behavior over the two monitored years (Fig. 5a). At the beginning of the monitoring

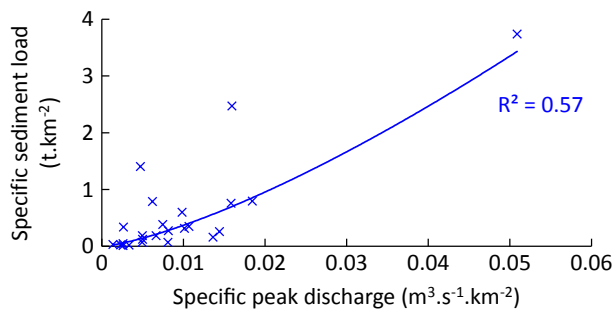


Fig. 8. Relationship between specific sediment load and specific peak discharge for the Bonnée river.

period, when the baseflow remained at a high level, suspended sediment concentration displayed regular peaks, in response to rainfall events. This period of significant transport lasted for several months, until early March 2018. Then, the subsequent sediment concentration peaks occurred mainly when rainfall events were significant and after long periods without high flow periods in the tile drain network. During the 2017–2018 hydrological year, suspended sediment loads ranged from 6×10^{-4} to 9 t.km^{-2} at the event scale for the tile drainage network (34 ha), while it was ranging from 1×10^{-3} to $2 \times 10^{-1} \text{ t.km}^{-2}$ during the 2018–2019 hydrological year. In addition to these fluxes, peak concentrations were also analyzed focusing on significant storm events, arbitrarily defined by suspended sediment concentrations higher than 250 mg.l^{-1} . Thirty events with such high concentrations were recorded during the 2017–2018 hydrological year while during the 2018–2019 hydrological year, with only 56% of the 2017–2018 cumulative rainfall, less than 20 of these high concentration events were recorded. However, relatively high peaks of suspended sediment concentrations were also observed during this 2018–2019 monitoring year. Over these two years, respectively 71% and 57% of the events displaying high suspended sediment concentration peaks were measured during winter, corresponding to periods of high flows. Moreover, during storm events, fast sediment transport – calculated during the fast peak of the rising limb in a similar way as it was performed for water in Section 3.2 – represented, on average, 15% of the sediment load. The concentrations measured in the tile drain network were in agreement with those found in other studies conducted at a tile drain outlet located in an agricultural catchment in a comparable environment in France (Grangeon et al., 2017). The high concentrations, along with the significance of fast transport from tile drains, highlight the potential major impact of tile drainage on the catchment sediment dynamics. A statistical analysis was performed on suspended sediment fluxes from the tile drainage network and those from the river (correlation table provided in supplementary material). For the Bonnée River catchment, it revealed that, among the variables analyzed (describing rainfall and flood event characteristics, see Section 2.6), the specific peak discharge correlated reasonably well with the specific sediment load of the Bonnée River catchment (Fig. 8).

The determination coefficient was higher using a linear relationship ($R^2 = 0.68$), but a power law is presented in this study, based on a previous study analyzing this relationship over multiple catchments (Duvert et al., 2012). However, for the tile drainage network, the relationship with the specific peak discharge was very variable in time, depending upon both the season and the monitored year. Indeed, no relationship was found during winter ($r = 0.40$) when the base flow was high, with the regular outflow of water from the drain pipes. It indicated that increase in peak flow, which should have resulted in increased transport capacity and therefore increased sediment fluxes, was limited by another factor that we hypothesized to be sediment storage between storm events, when water flow in drains was low. Accordingly, there was a clear progressive decrease in the specific suspended sediment load as winter progressed ($R^2 = 0.78$). It corresponded to a shift in the suspended sediment concentration dynamics (Fig. 5a) from high

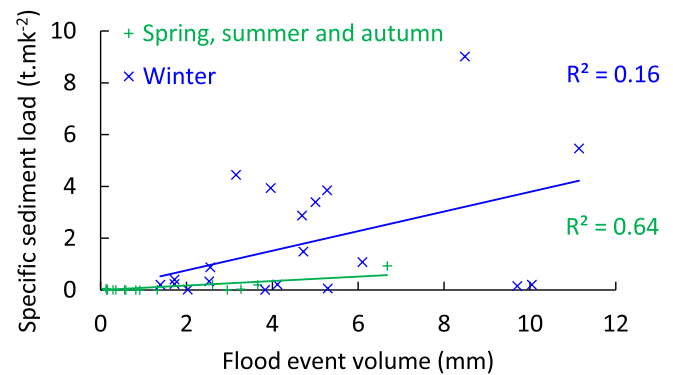


Fig. 9. Relationship between specific sediment load and rainfall depth, for winter (blue) and the other seasons (green) for the tile drain network. (For interpretation of the references to color in this figure legend, the reader is referred to the web version of this article.)

concentrations and regular sediment peaks to limited sediment concentrations and peaks. This result suggests that suspended sediments fluxes from the tile drain network were controlled by sediment storage and exhaustion in the tile drainage network, and its progressive evolution throughout the year.

The relationship between specific peak discharge and specific sediment load was good ($R^2 = 0.68$) for the tile drain network during spring, autumn and summer of the first monitored year (i.e. from March to December 2018). It corresponded to a decrease in the base flow, responding to a decreased water transfer and therefore a lower transport capacity through the soil column down to the pipes. We therefore hypothesized that sediment from tile drains was likely to accumulate, leaving stored sediment available for resuspension during the subsequent flood events.

During the second monitored year, alternating periods of relatively low or null base flow were observed, and associated suspended sediment loads remained very low: on average, over the two winter seasons, suspended sediment loads were 22 times lower in 2018–2019 compared to 2017–2018. This drop in sediment fluxes was also reflected by the low concentrations measured (Fig. 5), displaying only a few – although significant – suspended sediment concentration peaks. Most of these peaks occurred early in winter. Material accumulated during periods of ephemeral flow through the soil column allowed soil particles to be mobilized and transported to the drain network. This hypothesis may explain why, in the current research, a good relationship was not found between drain water flow and sediment load when considering the entire data set ($R^2 = 0.5$), which confirms results obtained by Chapman et al. (2005). Interestingly, this relationship was higher when tested separately for winter and for the other seasons (Fig. 9).

A large scattering was observed in the relationship between specific sediment load and rainfall depth ($R^2 = 0.16$) over the winter period, reflecting all the processes that may control sediment load: particle detachment and transfer over the soil column, sediment accumulation and subsequent erosion and the associated sediment selectivity. During the other seasons, when baseflow was low and when significant sediment loads remained episodic, the relationship between the specific sediment load and rainfall depth increased ($R^2 = 0.64$), reflecting a higher degree of connectivity, associated with a direct transfer of sediments with flowing water.

3.4. Limitations and implications of this study

In similar lowland drained catchments with gentle slopes, tile drains are usually immersed during flood events. The studied catchment configuration provided an original framework to isolate and analyze water and sediment fluxes from multiple tile drains throughout the year and in contrasted hydrological conditions (baseflow and flood events).

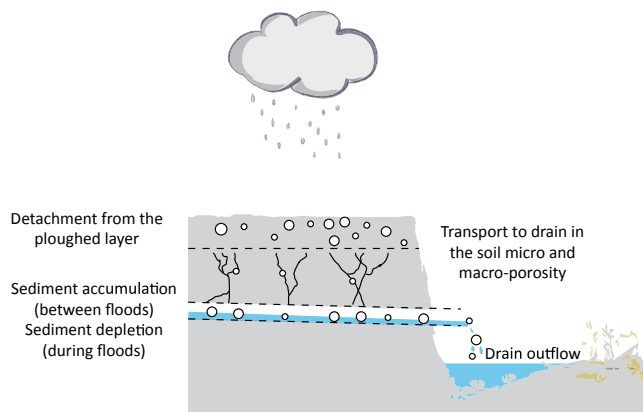


Fig. 10. Conceptual diagram of sediment transfers through tile drains.

However, due to this particular configuration, it was not possible to investigate in detail the interactions between river/ditches and tile drain flows, which are likely to occur in similar catchments. This could be usefully addressed in future investigations.

Moreover, the two studied years were either wet or dry. It offered contrasted conditions to study the tile drains dynamics, which should have provided data of the tile drain network functioning under “extreme” conditions. However, because only two monitoring years could be recorded, the effects of successive wet, mean or dry years could not be investigated. Therefore, monitoring tile-drained catchments over longer periods should provide valuable insights into tile drain dynamics, especially regarding the hypothesized processes of sediment storage and exhaustion. Medium to long-term water and sediment high-resolution monitoring is indeed extremely scarce in the literature (Esteves et al., 2019) and, to the best of our knowledge, do not exist in the case of tile drain.

The current study however used an original experimental set-up to measure water and sediment flow originating from tile drains, using high frequency monitoring. Such data sets, extremely scarce in the literature, provided insights into the hydrographs and sedigraphs generated from multiple drained plots under contrasted monitoring conditions including both a wet and a dry year. Based on this unique monitoring, a conceptual diagram of tile drain functioning is proposed (Fig. 10).

4. Conclusions

Water and suspended sediment dynamics were characterized during two hydrological years in a drained agricultural lowland catchment. A specific drainage collection network allowed the detailed quantification of water and sediment fluxes originating from a 34-ha surface area of drained fields. The results showed the very dynamic behavior of the tile drainage system. At the event scale, suspended sediment loads from the tile drains were significant, ranging from $6 \times 10^{-4} \text{ t}\cdot\text{km}^{-2}$ to $9 \text{ t}\cdot\text{km}^{-2}$. The occurrence of double transfer pathways in the tile drains, previously demonstrated in the literature although for individual plots, was confirmed in this study for multiple plots, suggesting that this process may be widely significant in tile-drained environments. Water and sediment fluxes occurring during the fast stages of tile drain flood events were calculated to be in the order of 15% of the total flood event fluxes. The data suggests that the succession of deposition and resuspension stages of sediment stored in the drainage network play a significant role on sediment dynamics in the tile drain system.

Although these results may reflect the behavior of an individual catchment, the original experimental set up allowed insights into the hydrographs and sedigraphs of multiple drained plots. In the future, the factors controlling the sediment storage originating from the cultivated topsoil layer to the tile drains during ephemeral flow conditions should

be further quantified, for instance through the measurement of short-lived fallout radionuclides characterized by contrasting half-lives (e.g. ^7Be , $^{210}\text{Pb}_{\text{xs}}$) or alternative low-cost measurements (e.g. color, magnetic susceptibility). Furthermore, the impacts of these transfers and their dynamics on sediment and contaminant exports from agricultural drained catchments should be further quantified in these lowland environments.

Declaration of Competing Interest

The authors declare that they have no known competing financial interests or personal relationships that could have appeared to influence the work reported in this paper.

Acknowledgments

The reviewers provided very detailed comments that greatly contributed to improve the manuscript. This work received financial support from the Loire-Brittany Water Agency in the framework of the Describe research project, under the supervision of Xavier Bourrain, Jean-Noël Gauthier and Anne Colmar. Anthony Foucher is warmly acknowledged for providing the artwork used in Fig. 10.

Appendix A. Supplementary data

Supplementary data to this article can be found online at <https://doi.org/10.1016/j.catena.2020.105033>.

References

- Akay, O., Fox, G.A., 2007. Experimental investigation of direct connectivity between macropores and subsurface drains during infiltration. *Soil Sci. Soc. Am. J.* 71 (5), 1600–1606.
- Beck, H.E., Zimmermann, N.E., McVicar, T.R., Vergopolan, N., Berg, A., Wood, E.F., 2018. Present and future Köppen-Geiger climate classification maps at 1-km resolution. *Sci. Data* 5, 180214.
- Blann, K.L., Anderson, J.L., Sands, G.R., Vondracek, B., 2009. Effects of agricultural drainage on aquatic ecosystems: a review. *Crit. Rev. Environ. Sci. Technol.* 11, 909–1001.
- Cerdan, O., Souchère, V., Lecomte, V., Couturier, A., Le Bissonnais, Y., 2002. Incorporating soil surface crusting processes in an expert-based runoff model: sealing and Transfer by Runoff and Erosion related to Agricultural Management. *Catena* 46, 189–220.
- Chapman, T.G., 1991. Comment on “Evaluation of automated techniques for base flow and recession analyses”. *Water Resour. Res.* 27, 1483–1484.
- Chapman, A.S., Foster, I.D.L., Lees, J.A., Hodgkinson, R.A., 2005. Sediment delivery from agricultural lands to rivers via subsurface drainage. *Hydrol. Process.* 19, 2875–2897.
- Collins, A.L., Pulley, S., Foster, I.D.L., Gellis, A., Porto, P., Horowitz, A.J., 2017. Sediment source fingerprinting as an aid to catchment management: a review of the current state of knowledge and a methodological decision-tree for end-users. *J. Environ. Manage.* 194 (1), 86–108.
- Cooper, R.J., Krueger, T., Hiscock, K.M., Rawlins, B.G., 2015. High-temporal resolution fluvial sediment source fingerprinting with uncertainty: a Bayesian approach. *Earth Surf. Proc. Land.* 40, 78–95.
- De Girolamo, A.M., Pappagallo, G., Lo, Porto A., 2015. Temporal variability of suspended sediment transport and rating curves in a Mediterranean river basin: the Celone (SE Italy). *Catena* 128, 135–143.
- De Vente, J., Poesen, J., 2005. Predicting soil erosion and sediment yield at the basin scale: scale issues and semi-quantitative models. *Earth Sci. Rev.* 71, 95–125.
- Deasy, C., Brazier, R.E., Heathwaite, A.L., Hodgkinson, R., 2009. Pathways of runoff and sediment transfer in small agricultural catchments. *Hydrol. Process.* 23, 1349–1358.
- Delmas, M., Pak, L.T., Cerdan, O., Souchère, V., Le Bissonnais, Y., Couturier, A., Sorel, L., 2012. Erosion and sediment budget across scale: a case study in a catchment of the European loess belt. *J. Hydrol.* 420–421, 255–263.
- Duvert, C., Nord, G., Gratiot, N., Navratil, O., Nadal-Romero, E., Mathys, N., Némery, J., Regüés, D., García-Ruiz, J.M., Gallart, F., Esteves, M., 2012. Towards prediction of suspended sediment yield from peak discharge in small erodible mountainous catchments (0.45–22 km²) of France, Mexico and Spain. *J. Hydrol.* 454–455, 42–55.
- Esteves, M., Legout, C., Navratil, O., Evrard, O., 2019. Medium term high frequency observation of discharges and suspended sediment in a Mediterranean mountainous catchment. *J. Hydrol.* 568, 562–574.
- Evrard, O., Vandaele, K., Bielders, C., Wesemael, B., 2008. Seasonal evolution of runoff generation on agricultural land in the Belgian loess belt and implications for muddy flood triggering. *Earth Surf. Proc. Land.* 33, 1285–1301.
- Evrard, O., Nord, G., Cerdan, O., Souchère, V., Le Bissonnais, Y., Bonté, P., 2010. Modelling the impact of land use change and rainfall seasonality on sediment export

- from an agricultural catchment of the northwestern European loess belt. *Agric. Ecosyst. Environ.* 138, 83–94.
- Fiener, P., Wilken, F., Auerswald, K., 2019. Filling the gap between plot and landscape scale – eight years of soil erosion monitoring in 14 adjacent watersheds under soil conservation at Scheyern, Southern Germany. *Adv. Geosci.* 48, 31–48.
- Foucher, A., Lacey, P.J., Salvador-Blanes, S., Evrard, O., Le Gall, M., Lefevre, I., Cerdan, O., Rajkumar, V., Desmet, M., 2015. Quantifying the dominant sources of sediment in a drained lowland agricultural catchment: the application of a thorium-based particle size correction in sediment fingerprinting. *Geomorphology* 250, 271–281.
- Frey, S.K., Hwang, H.T., Park, Y.J., Hussain, S.I., Gottschall, N., Edwards, M., Lapen, D. R., 2016. Dual permeability modelling of tile drain management influences on hydrologic and nutrient transport characteristics in macroporous soil. *J. Hydrol.* 535, 392–406.
- Grangeon, T., Manière, L., Foucher, A., Vandromme, R., Cerdan, O., Evrard, O., Pene-Galland, I., Salvador-Blanes, S., 2017. Hydro-sedimentary dynamics of a drained agricultural catchment: a nested monitoring approach. *Vadose Zone J.* 16 (12) <https://doi.org/10.2136/vzj2017.05.0113>.
- Haddachi, A., Ryder, D.S., Evrard, O., Olley, J., 2013. Sediment fingerprinting in fluvial systems: a review of tracers, sediment sources and mixing models. *Int. J. Sedim. Res.* 28, 560–578.
- Hansen, A.L., Refsgaard, J.C., Christensen, B.S.B., Jensen, K.H., 2013. Importance of including small-scale tile drain discharge in the calibration of a coupled groundwater-surface water catchment model. *Water Resour. Res.* 49, 585–603.
- Kemp, P., Sear, D., Collins, A., Naden, P., Jones, I., 2011. The impact of fine sediment on riverine fish. *Hydrol. Process.* 25, 1800–1821.
- King, K.W., Fausey, N.R., Williams, M.R., 2014. Effects of subsurface drainage on streamflow in an agricultural headwater watershed. *J. Hydrol.* 519, 438–445.
- Kladivko, E.J., Van Scoyoc, G.E., Monke, E.J., Oates, K.M., Pask, W., 1991. Pesticide and nutrient movement into subsurface tile drains on a silt loam soil in Indiana. *J. Environ. Qual.* 20, 264–270.
- Kladivko, E.J., Brown, L.C., Baker, J.L., 2001. Pesticide transport to subsurface tile drains in humid regions of North America. *Crit. Rev. Environ. Sci. Technol.* 34, 608–620.
- Le Bissonnais, Y., Lecomte, V., Cerdan, O., 2004. Grass strip effects on runoff and soil loss. *Agronomie* 24, 129–136.
- Le Gall, M., Evrard, O., Foucher, A., Lacey, J.P., Salvador-Blanes, S., Maniere, L., Lefevre, I., Cerdan, O., Ayrault, S., 2017. Investigating the temporal dynamics of suspended sediment during flood events with ^{7}Be and $^{210}\text{Pb}_{\text{xs}}$ measurements in a drained lowland catchment. *Sci. Rep.* 7, 42099. <https://doi.org/10.1038/srep42099>.
- Li, H., Sivapalan, M., Tian, F., Liu, D., 2010. Water and nutrient balances in a large tile-drained agricultural catchment. *Hydrol. Earth Syst. Sci.* 14 (11), 2259–2275.
- Macrae, M.L., English, M.C., Schiff, S.L., Stone, M., 2007. Intra-annual variability in the contribution of tile drains to basin discharge and phosphorus export in a first-order agricultural catchment. *Agric. Water Manag.* 92, 171–182.
- Meybeck, M., Laroche, L., Dürr, H.H., Syvitski, J.P.M., 2003. Global variability of daily total suspended solids and their fluxes in rivers. *Global Planet. Change* 39, 65–93.
- Montagne, D., Cornu, S., Le Forestier, L., Cousin, I., 2009. Soil drainage as an active agent of recent soil evolution: a review. *Pedosphere* 19 (1), 1–13.
- Muma, M., Rouseau, A.N., Gumiere, S.J., 2016. Assessment of the impact of subsurface agricultural drainage on soil water storage and flows of a small watershed. *Water* 8 (326). <https://doi.org/10.3390/w8080326>.
- Nagy, D., Rosenborm, A.E., Iversen, B.V., Plauborg, F., 2020a. Effects of preferential transport and coherent denitrification on leaching of nitrate to drainage. *Hydrol. Earth Syst. Sci.* <https://doi.org/10.5194/hess-2019-666>, under review.
- Nagy, D., Rosenborm, A.E., Iversen, B.V., Jabloun, M., Plauborg, F., 2020b. Estimating the degree of preferential flow to drainage in an agricultural clay till field for a 10-year period. *Hydrol. Earth Syst. Sci.* <https://doi.org/10.5194/hess-2019-665>, under review.
- Navratil, O., Esteves, M., Legout, C., Gratiot, N., Némery, J., Willmore, S., Grangeon, T., 2011. Global uncertainty analysis of suspended sediment monitoring using turbidimeter in a small mountainous river catchment. *J. Hydrol.* 398, 246–259.
- Owens, P.N., Batalla, R.J., Collins, A.J., Gomez, B., Hicks, D.M., Horowitz, A.J., Kondolf, G.M., Marden, M., Page, M.J., Peacock, D.H., Petticrew, E.L., Salomons, W., Trustrum, N.A., 2005. Fine-grained sediment in river systems: environmental significance and management issues. *River Res. Appl.* 21 (7), 693–717.
- Øygarden, L.J., Jenssen, P.D., 1997. Soil erosion via preferential flow to drainage systems in clay soil. *Geoderma* 76 (1–2), 65–86.
- Peel, M.C., Finlayson, B.L., McMahon, T.A., 2007. Updated world map of the Köppen-Geiger climate classification. *Hydrol. Earth Syst. Sci.* 11, 1633–1644.
- Rozemeijer, J.C., van der Velde, Y., van Geer, F.C., Bierkens, M.F.P., Broers, H.P., 2010. Direct measurements of the tile drain and groundwater flow route contributions to surface water contamination: from field-scale concentration patterns in groundwater to catchment-scale surface water quality. *Environ. Pollut.* 158, 3571–3579.
- Russell, M.A., Walling, D.E., Hodgkinson, R.A., 2001. Suspended sediment sources in two small lowland agricultural catchments in the UK. *J. Hydrol.* 252, 1–24.
- Saffarpour, S., Western, A.W., Adams, R., McDonnell, J.J., 2016. Multiple runoff processes and multiple thresholds control agricultural runoff generation. *Hydrol. Earth Syst. Sci.* 20, 4525–4545.
- Souchère, V., King, C., Dubreuil, N., Lecomte-Morel, V., Le Bissonnais, Y., Chalot, M., 2003. Grassland and crop trends: role of the European Union Common Agricultural Policy and consequences for runoff and soil erosion. *Environ. Sci. Policy* 6, 7–16.
- Spaling, H., Smit, B., 1995. Conceptual model of cumulative environmental effects of agricultural land drainage. *Agric. Ecosyst. Environ.* 53, 299–308.
- Stone, W.W., Wilson, J.T., 2006. Preferential flow estimates to an agricultural tile drain with implications for glyphosate transport. *J. Environ. Qual.* 35, 1825–1835.
- Tournebise, J., Henine, H., Chaumont, C., 2020. Gérer les eaux de drainage agricole: du génie hydraulique au génie écologique ». *Sciences Eaux & Territoires* 32, 32–40. <https://doi.org/10.14758/SET-REVUE.2020.2.06>.
- Turtola, E., Alakukku, L., Uusitalo, R., Kaseva, A., 2007. Surface runoff, subsurface drainflow and soil erosion as affected by tillage in a clayey Finnish soil. *Agric. Food Sci.* 16, 332–351.
- Turunen, M., Warsta, L., Paasonen-Kivekäs, M., Nurminen, J., Myllys, M., Alakukku, L., Äijö, H., Puustinen, M., Koivusalo, H., 2013. Modelling water balance and effects of different subsurface drainage methods on water outflow components in a clayey agricultural field in boreal conditions. *Agric. Water Manag.* 121, 135–148.
- Turunen, M., Warsta, L., Paasonen-Kivekäs, M., Koivusalo, H., 2017. Computational assessment of sediment balance and suspended sediment transport pathways in subsurface drained clayey soils. *Soil Tillage Res.* 174, 58–69.
- Ulén, B., Persson, K., 1999. Field-scale phosphorous losses from a drained clay soil in Sweden. *Hydrol. Process.* 13, 2801–2812.
- Ulén, B., Gunborg, A., Kreuger, J., Svanbäck, A., Etana, A., 2012. Particulate-facilitated leaching of glyphosate and phosphorous from a marine clay soil via tile drain. *Acta Agriculturae Scandinavica*. <https://doi.org/10.1080/09064710.2012.697572>.
- Uusitalo, R., Turtola, E., Kauppi, T., Lilja, T., 2001. Particulate phosphorous and sediment in surface runoff and drainflow from clayey soils. *J. Environ. Qual.* 30, 589–595.
- Van Den Bogaert, R., Labile, J., Cornu, S., 2013. Aggregation and dispersion behavior in the 0–2- μm fraction of Luvisols. *Soil Sci. Soc. Am. J.* 79, 43–54.
- Vincent, B., 2020. Principes techniques et chiffres du drainage agricole – De la tuyautique à l’hydro-diplomatie. *Sciences Eaux & Territoires* 32, 8–15. <https://doi.org/10.14758/SET-REVUE.2020.2.02>.
- Walling, D.E., Russell, M.A., Hodgkinson, R.A., Zhang, Y., 2002. Establishing sediment budgets for two small lowland agricultural catchments in the UK. *Catena* 37, 323–353.
- Walling, D.E., Collins, A.L., 2008. The catchment sediment budget as a management tool. *Environ. Sci. Policy* 11, 136–143.
- Warsta, L., Taskinen, A., Koivusalo, Paasonen-Kivekäs M., Karvonen, T., 2013. Modelling soil erosion in a clayey, subsurface-drained agricultural field with a three-dimensional FLUSH model. *J. Hydrol.* 498, 132–143.